

PCCP

Physical Chemistry Chemical Physics

Accepted Manuscript

This article can be cited before page numbers have been issued, to do this please use: M. Miroshnichenko and P. Bharmoria, *Phys. Chem. Chem. Phys.*, 2026, DOI: 10.1039/D5CP04142B.



This is an Accepted Manuscript, which has been through the Royal Society of Chemistry peer review process and has been accepted for publication.

Accepted Manuscripts are published online shortly after acceptance, before technical editing, formatting and proof reading. Using this free service, authors can make their results available to the community, in citable form, before we publish the edited article. We will replace this Accepted Manuscript with the edited and formatted Advance Article as soon as it is available.

You can find more information about Accepted Manuscripts in the [Information for Authors](#).

Please note that technical editing may introduce minor changes to the text and/or graphics, which may alter content. The journal's standard [Terms & Conditions](#) and the [Ethical guidelines](#) still apply. In no event shall the Royal Society of Chemistry be held responsible for any errors or omissions in this Accepted Manuscript or any consequences arising from the use of any information it contains.

ARTICLE

Received 00th January 20xx,
Accepted 00th January 20xx

DOI: 10.1039/x0xx00000x

Neat Ionic liquids and Deep Eutectic Solvents in Photonics: Status Quo and Future Directions

Mila Miroshnichenko,^a Pankaj Bharma,^{a,b*}

In the past decades, Ionic liquids (ILs) and deep eutectic solvents (DESs) have gained recognition as green solvents, mainly because of their low vapor pressure, potential for recycling, and customized synthesis. The customization leverages task specificity for a particular application. While the photoactive ILs and DESs have been used as an adjuvant in aqueous or organic solution for a variety of applications, this perspective article discusses the relatively underexplored applications of neat ILs or DESs in the field of photonics. Specifically, customization of their chemical structure is discussed to facilitate a particular linear and non-linear optical response, serving as a solvent-free photonic component, including future directions.

Introduction

Ionic liquids (ILs), followed by deep eutectic solvents (DES) have emerged as potential green solvents in the past two decades for multitude applications ranging from separation and purification,^{1,2} protein-stability,³⁻⁵ energy,⁶⁻⁷ pharmaceuticals,⁸⁻⁹ biotransformation,^{10,11} detergency,¹² metal processing,¹³ and electrochemistry.^{14,15} This can be attributed to their properties including low vapour pressure, broad thermal ranges, recycling, biodegradability, specific solvation, and customized easy synthesis.^{16,17} Neat ILs are salts comprising discrete organic cation associated with a discrete organic or inorganic anion via weak electrostatic, H-bonding or London dispersion interactions below 100 °C.¹⁸ Neat DESs consist of a eutectic mixture formed by Lewis or Brønsted acids and bases, which may encompass a diverse range of anion and/or cations. The liquidity of DESs at or near the room temperature supported by hydrogen bond interactions between the Lewis or Brønsted acid (donor), and Lewis base (acceptor).¹⁹ While both ILs and DESs share similar physical properties, difference in their chemical properties contribute to the applications in diverse fields.²⁰ Photonics is one such field which need specificity of the chemical nature of ILs or DESs. This is due to the fact that photonics involves the generation, detection, and manipulation of light; therefore, ions with a specific chemical structure can absorb, emit, and scatter the light. While both ILs and DESs offer advantage of the customization of the chemical structure, they have been underexplored in the field of photonics as a neat-solvents. This perspective article discusses the limited work reported in relation to the specific chemical structure of ILs or DESs components, as well as

their implications in future linear and non-linear optical applications. For better understanding of the cross-disciplinary readership ILs and DESs and linear and non-linear optics are briefly described before main discussion

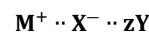
Ionic liquid and Deep Eutectic Solvent

An Ionic liquid can be simply described by the following formula.



Where **M**⁺ and **X**⁻ are discrete cation or anions associated mainly via weak electrostatic interactions due to steric hindrance caused by the organic cation or anion moiety.²¹ For example, imidazolium cation based ILs; [C₄mim]⁺Cl⁻ (m.p. \approx 70°C)²² or [C₄mim]⁺[C₈OSO₃]⁻ (m.p. \approx 37°C).²³ Here, replacement of Cl⁻ by a bulky [C₈OSO₃]⁻ creates steric hindrance to weaken the electrostatic interactions thereby decreasing the melting point (m.p.) see Figure 1a. There are tens of discrete cations and anions which can be customized and combined in several combinations to obtain thousands of ILs, details of which can be availed from the cited references.²⁴

A deep eutectic solvent is a eutectic mixture with a lower melting temperature than that of its constituent components. It can be described by following formula.²



Where **M**⁺ is generally a nonsymmetric cation, **X**⁻ is Lewis base and **Y** is a Lewis or Brønsted acid with a number *z*. For example, mixing [Cho]Cl (m.p. \approx 303°C) and NH₂CONH₂ (m.p. \approx 134°C) in 1:2 molar ratio leads to the formation of DES; [Cho]⁺·Cl⁻·₂HNCONH₂ with a lowered freezing temperature (T_f \approx 12°C) due to hydrogen bond interaction of urea with Cl⁻ (See Figure 1b).²⁶ DESs can be of type I to IV depending on their structure, the details of which can be availed from the following cited references.²⁷

^a The Institute of Materials Science of Barcelona, ICMAB-CSIC, 08193, Bellaterra. Barcelona, Spain

^b Department of Chemical Engineering, Universitat Politècnica de Catalunya, EEBE, Eduard Maristany 10–14, 08019 Barcelona, Spain.

* Footnotes relating to the title and/or authors should appear here.

ARTICLE

Journal Name

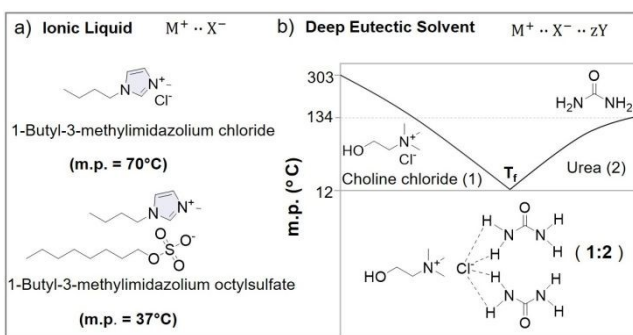


Figure 1. Chemical equations and molecular structures of a) Ionic liquids and b) deep eutectic solvent.

Linear and Non-linear Optics

In linear optics, an incident light wave (generally weak) causes vibration of a molecule, followed by the emission of a light wave having the same frequency as the incident light (Figure 2A). Therefore, linear optics follows the superposition principle; $A+B = X+Y$,²⁸ where A and B are input light waves hitting the molecule giving output light waves X and Y with the same frequency. Under the application of weak electric field, the loosely bonded electrons in the materials undergo slight displacement from their equilibrium

position to induce an electric dipole moment ($\vec{P}(t)$). Since electrons near the nucleus are bound more strongly, their displacement potential is approximated as harmonic. Therefore, as per the harmonic approximation, the \vec{P} scales linearly with the electric field (\vec{E}) amplitude of the incident light as per the following equation 1.^{28, 29}

$$\vec{P}(t) = \epsilon_0 \chi \vec{E}(t) \quad (1)$$

Where \vec{P} is induced dipole moment per unit volume, ϵ_0 is the permittivity of the free space, χ is polarization susceptibility. The common linear optical properties are reflection, refraction, scattering, and diffraction etc.

In non-linear optics, an intense light wave upon interaction with the molecule changes its optical properties such as frequency (Figure 2B). Non-linear optics does not follow the superposition principle; $A+B \neq X+Y$, hence the optical properties like frequency, polarization and phase of the incident light undergoes change as the polarization density of the medium reacts non-linearly to the electric field of the light. Non-linearity is displayed by the molecules when the electric field strength of the light is high compared to the intra-atomic electric field *i. e.* $E_a \approx 2 \times 10^7$ electrostatic unit.

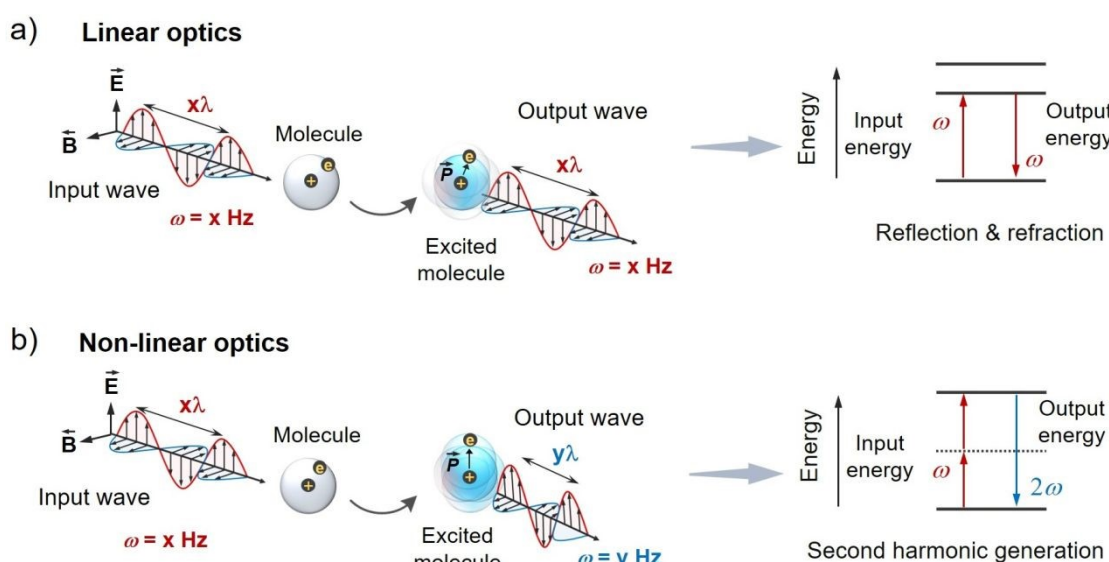


Figure 2. Illustration of a) linear and b) non-linear optical response of a molecule upon excitation with a linearly polarized light wave. λ = wavelength; ω = frequency of the light wave.

Due to the strong electric field, the binding potential of electrons near the nucleus cannot be approximated as harmonic, resulting in large displacements from the equilibrium position. Therefore, the electron displacement does not scale linearly with the electric field as the non-linear electron motions become more significant. Hence, the induced polarization in non-linear optics is defined by the equation 4.³⁰

$$\vec{P}_{NL} = \chi^{(1)} \vec{E} + \chi^{(2)} \vec{E}^2 \chi^{(3)} \vec{E}^3 + \dots \quad (2)$$

Where $\chi^{(1)}$ is the linear polarization susceptibility of the materials and $\chi^{(2)}$ and $\chi^{(3)}$ are non-linear polarization susceptibility of the materials corresponding to the second and third order effects such as second and third harmonic generation, two or three photon

absorption, triplet-triplet annihilation photon upconversion, and stimulated Raman scattering etc. Both NILs and DESs show different linear and non-linear optical response compared to other solvents. This is due to their unique ionic nature, charge delocalization, customized heterogeneous polarity, and local microviscosity.

Heterogeneity, Polarity and Viscosity of Ionic Liquids and Deep Eutectic Solvents

During the light-matter interaction in solution, the solvent polarity and viscosity play a crucial role in altering the photonic properties by influencing the electronic transitions and molecular dynamics.³¹ The probability of electronic transition between different quantum states

can be measured using the transition dipole moment integral equation 5.³²

$$\langle \mu \rangle_T = \int \psi_a^* \hat{\mu} \psi_b \, d\mathbf{r} = \mu_T \quad (3)$$

Where $\langle \mu \rangle_T$ is the expectation value of transition dipole moment vector ($\hat{\mu}$) between the quantum states ψ_a^* and ψ_b , integrated over all coordinates, $d\mathbf{r}$. If $\mu_T \neq 0$, transition is allowed (e.g. singlet to singlet transition), and when $\mu_T = 0$, transition is forbidden (e.g. singlet to triplet transition). The solvent polarity affects the transition dipole moment indirectly by altering the electronic distribution in the molecule in the ground and excited state, which affects its interaction with light through induced polarization as per equation 3, 4 and 5 (Figure 2). The nanoscale heterogeneity of ILs separates the ions into distinct polar and non-polar domains.³³⁻³⁴ Polar domains are formed by charged headgroups of cations and anions, stabilized by electrostatic and hydrogen-bonding interactions, whereas non-polar domains are formed by aggregation of alkyl chains due to van der Waal's interactions (Figure 3).³⁵

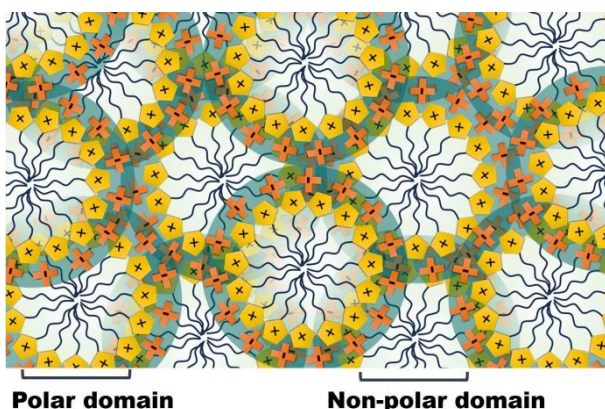


Figure 3. Illustration of the segregated polar and non-polar domain in neat ILs. The domain length varies with an increase in the size of cation or anion headgroup and their alkyl chain length.

More importantly the length and structure of diversity of the polar/non-polar domain can be altered by changing molecular structure of the cation or anion and their alkyl chain length.³⁶⁻³⁷ For instance, the domain structure can vary from spatial heterogeneous to liquid crystalline with an increase in the alkyl chain length.³⁶ The distinct structure, local environment, diffusion, reorientation and association dynamics of ILs ions in different domains play a key role in governing optical properties of theirs or of the molecules dissolved in them.³⁸⁻⁴¹ This is because the variations in polarity across domains alters the stability of ground and excited state of molecule due to different interaction energy of the solvent dipoles with the dipoles of excited chromophores leading to inhomogeneous spectral broadening and bathochromic or hypsochromic spectral shifts.⁴² Similar to NILs, DESs also possesses differential polarity due to the heterogeneity in their structure which varies with the structure of their constituents.⁴³⁻⁴⁶ The differential polarity can also affect the molecular solubility of chromophores to influence the absorption coefficients and emission lifetimes between different states.⁴⁷ The differential polarity of NILs and DESs can be investigated using Kamlet-Taft's solvent parameters (α , β and π^*) using standard equations.⁴⁸⁻⁵⁰ These parameters denote hydrogen bond donor capacity (α), hydrogen bond acceptor capacity (β), and polarizability (π^*) of the liquid. The Kamlet-Taft's parameters can be used to design ILs/DESs or their binary mixtures with specific polarity for a specific photonic application in the liquid-state. This is because the change in α , β and π^* affects both the solvation and diffusion of the

dissolved chromophores, which affects both excited-state dynamics (monomer vs excimer emission) and energy transfer.⁵¹⁻⁵⁴ For example, aggregation induced emission enhancement (AIE), or quenching which are highly sensitive to solvent polarity.⁵⁴⁻⁵⁷ In case of AIE the molecular motions (rotation and vibrations) ceases due to the packing of molecules in a certain geometry, which blocks the non-radiative decay (k_{nr}) to boost the radiative decay (k_r) to enhance the fluorescence quantum yield (Φ_f) according to the following relation 4.

$$\Phi_f = \frac{k_r}{k_r + k_{nr}} \quad (4)$$

While AIE is specific to certain type of molecules, most of the chromophores show quenching of fluorescence due to aggregation induced by the change in concentration and solvent polarity. This is as per Kasha rule which states that a small change in distance (R) and angle (θ) between the transition dipole moment (μ) of neighbouring molecules in a medium of certain dielectric constant (ϵ) alters their inter-electronic coupling (J) according to the following relation 5.⁵⁸

$$J = \frac{\mu^2 (1 - 3 \cos^2 \theta)}{4 \pi \epsilon R^2} \quad (5)$$

The close packing of dyes due to aggregation results in coupling to produce new electronic states like excimers with bathochromic or hypsochromic shift in the optical spectra with the quenching of fluorescence. Therefore, polarity and solvent chromophore interactions control's chromophores aggregation due to solvophobic effect that can either lead to enhancement and quenching of fluorescence as per the type of the dissolved molecule.⁵⁹ That is why the understanding of the Kamlet-Taft's parameters is important for designing the photoactive of NILs or DESs. The issue of photoluminescence quenching can be addressed by the introduction of the fluorophore as a constituent of either NILs or DESs which can control the intermolecular interactions and solvophobicity by judicious choice of the counter ions. The suitable packing or co-assembly of molecules in such systems can maintain a specific angular distance to avoid excimer formation.⁶⁰

Viscosity is another key property which influence the photonic properties of molecules by controlling the polarization, diffusion of chromophores and oxygen. The viscosity (η) is related to diffusion coefficient of a molecule (D) via Stokes-Einstein equation 6.⁶¹

$$D = \frac{k_B T}{6 \pi \eta R} \quad (6)$$

Where $k_B T$ is Boltzmann constant at a specific temperature (T), and R is the radius of the a generally considered spherical particle in the solution. The higher viscosity tends to inhibit the non-radiative decay by restricting the collisions between the molecules and with ground state oxygen (triplet) thereby increasing the emission lifetimes and photo-stability.⁶² The heterogeneous structure of ILs or DESs changes with the change in alkyl chain, which alters the local bulk and shear moduli of the non-polar domains eventually altering the exciton diffusion.⁶³⁻⁶⁴ Therefore, viscosity effects in both ILs and DESs can highly domain specific as the dissolved molecule mostly experiences the local environment.⁶⁵⁻⁶⁶ The understanding of the microviscosity is specifically important for the applications of ILs or DESs in photon upconversion processes involving triplet-state.⁶⁷⁻⁶⁸ This is because the chromophore triplets can be quenched by the diffusing molecular oxygen which exist in triplet-ground state. The higher local microviscosity can reduce diffusion of triplet-oxygen to enhance upconversion performance.⁶⁹⁻⁷⁰ Since the viscosity affect the molecular polarization via dielectric relaxation time and bimolecular



ARTICLE

Journal Name

reaction rates via molecular collisions, it affects most of the diffusion dependent and solute-solvent interactions based optical processes.⁷¹⁻⁷⁵ Hence, understanding of the viscosity of NILs and DESs is important for their photonics applications. Details related to alteration in viscosity of both ILs and DESs due to the change in chemical structure can be availed from the following references.⁷⁶⁻⁷⁷

View Article Online
DOI: 10.1039/D5CP04142B

Table 1. Summary of Neat Ionic liquids and Deep Eutectic Solvents and their Specific Property Exploited for Photonics

Neat Ionic Liquid	Photonic Property	Properties of NIL Exploited
[C ₂₋₈ mim] ⁺ [BF ₄] ⁻ and [C ₄ mim] ⁺ [PF ₆] ⁻	Optical absorption and emission	Customization, and polarity ⁸⁴
[C _n mim] ⁺ [X] ⁻ (n = 2, 4, 8; X = Cl, BF ₄ , PF ₆)	Red edge effect	Heterogeneity, polarity and viscosity ^{88-90,93}
[C _n mpy] ⁺ [X] ⁻ (n = 3, 4, 8; X = BF ₄ , N(CN) ₂)		
[C _{nR} mim] ⁺ [I] ⁻ (R = diphenylacrylonitrile; n=1, 7, 11)	Circularly Polarized Luminescence	Structural customization, Chirality ^{94-95, 97}
[C ₂ TCBNim] ⁺ [PF ₆] ⁻ , [(C ₄) ₄ N] ⁺ [X] ⁻ (X = Pro, Val, Asp)		
[C ₁₄ (C ₆) ₃ P] ⁺ [PbX ₄] ⁻ , [(C ₄) ₄ P] ⁺ [PbX ₄] ⁻	Neutron Scintillation	Proton richness, viscosity, low scattering ⁹⁹
[C ₁₄ (C ₆) ₃ P] ⁺ [X] ⁻ (X = HP-SO ₃ , C ₁₂ -FL)	Förster resonance energy transfer	Structure customization, Viscosity, Polarity ¹⁰⁰
[C ₁₄ (C ₆) ₃ P] ⁺ [DPASO ₃] ⁻ , [C ₁₄ (C ₂) ₃ P] ⁺ [DPASO ₃] ⁻	Dexter energy transfer in TTA-based photon upconversion	Structure customization, Heterogeneity, Viscosity, Thermal stability, Polarity ¹⁰¹⁻¹⁰⁴
[C ₁₄ (C ₆) ₃ P] ⁺ [PPOSO ₃] ⁻		
[C ₂ mim] ⁺ [N(CN) ₂] ⁻ , [X] ⁺ [NTf ₂] ⁻ (X = C ₄ mPyr, C ₄ Pyr)	Stimulated Raman scattering based photon up and down conversion	Structure customization, thermal stability ¹⁰⁵
[C ₄ mim] ⁺ [PF ₆] ⁻		
[C _n mim] ⁺ [X] ⁻ (n = 1 or 4; X = NTf ₂ , BF ₄ , ClO ₄ , PF ₆ , N(CN) ₂)	Gain medium in microfluidic dye laser operational via whispering gallery modes	Refractive index, and viscosity ¹⁰⁶
[C ₂ mim] ⁺ [C ₂ OSO ₃] ⁻	Electro-optical modulation	Conductivity, viscosity, electrochromic window ¹⁰⁹
[C ₄ mim] ⁺ [PF ₆] ⁻ and [C ₄ mim] ⁺ [BF ₄] ⁻	Reflectance	Liquidity, refractive index, surface tension, low vapour pressure, broad thermal range ^{110,112}
	Diffraction	Heterogeneity, polarizability, viscosity ¹¹⁷⁻¹¹⁸
Neat Deep Eutectic Solvent	Photonic Property	Properties of DES Exploited
[Cho] ⁺ [Cl] ⁻ : lactic acid	Negative non-liner refraction due to thermal lensing effect	Negative refractive index, heterogeneity, liquidity ¹²¹
Heptyltriphenylphosphine bromide: decanoic acid	Fluorescence	Structural customization, polarity ¹²⁴
[C ₄) ₄ N] ⁺ Cl ⁻ : zY (zY = D-(+)- α -glucose; D-(+)- β -glucose; L-(+)- α -glucose; D-(+)- β -fructose).	Circularly Polarized Luminescence	Structural customization, Chirality ¹²⁵⁻¹²⁷
[C ₄) ₄ N] ⁺ Cl ⁻ : zY: zY or [Cho]Cl: zY (zY = L-lactic acid, L-leucic acid, L-ascorbic acid, R/S-acetoxypyropionic acid, and methyl-(S)-lactate). [C ₄) ₄ N] ⁺ Cl ⁻ or [C ₄) ₄ P] ⁺ Cl ⁻ : zY (zY = L-or D-glutamic acid, L-proline, and L-arginine).		
[C _n) ₄ N] ⁺ Cl ⁻ : decanoic acid (n = 4 or 8)	Dexter energy transfer in TTA-based photon upconversion	Liquidity, polarity, thermal stability ¹²⁸
[M] ⁺ [X] ⁻ : zY (M = [(C ₂) ₄ N or Cho; X = Cl or Br; zY = ethylene glycol, or Glycine or Urea or tetraethylene glycol)	Excited-state proton transfer	Hydrogen bond acidity, Liquidity, nano-heterogeneity and polarity ¹³⁰⁻¹³¹

Neat Ionic Liquids as Photonic Component

The customized nature of ILs, leverage the possibility of engineering the chemical structures of both cation and anions for responding to the light waves of a specific energy due to electric field polarization.⁷⁸ However, the question, that what happens to NILs upon exposure to electromagnetic radiation of a specific wavelength is a key aspect of their photonic application,⁷⁹ considering the change in structural heterogeneity,⁸⁰ formation of possible transient photoexcited

species,⁸¹⁻⁸² and change in properties of input wave.⁸³ The most common IL cation imidazolium; [C_nmim]⁺ paired with an optically less active anion leverage an inherent optical property in the broad UV-blue region.⁸⁴ The neat [C_nmim]⁺ paired with BF₄⁻ anion show absorption maxima at ~160 and 210 nm with tail extending into the 400 nm range.⁸⁴ However, their emission spectra display excitation wavelength dependent red shift of the photoluminescence, known as the “Red Edge Effect (REE) (Figure 4a).”⁸⁵⁻⁸⁶

ARTICLE

Red Edge Effect

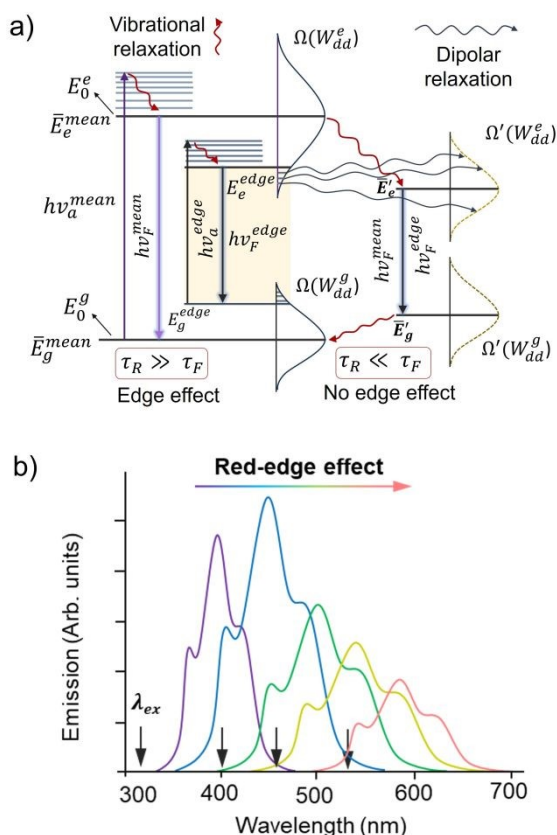


Figure 4. a) Illustration of the modified Jablonski diagram showing electronic transitions, vibrational and dipolar relaxation during red edge effect due to photoselection of certain chromophores experiencing different electric field due to the interactions of dipoles of excited chromophores with the solvent dipole when excited at the edge of absorption spectrum. b) Illustration of change in emission spectrum during red-edge effect with a change in the excitation energy. Figure 4a adapted from ref 87 with permission from [Elsevier B.V.] [Demchenko, *Biophys. Chem.*, 1982, 15, 101-10987], copyright 1982.

In REE the emission spectra undergo red-shift when excitation is performed at a long wavelength slope (Figure 4a-b). The REE is generally observed in condensed inhomogeneous medium with high polarity and restricted motion, like at low temperature or at high viscosity where dielectric relaxation slows down with a shift to low frequency and longer relaxation times (τ_R).⁸⁵⁻⁸⁶ In a typical case chromophore whose dipole moment and dipole orientation changes in the excited state (μ_e) with respect to ground state (μ_g) show REE due to the interactions of medium dipole (μ_m) with the chromophore's dipoles (dipolar interactions). As a result, the chromophore experiences different electric field with an added energy contribution from dipole-dipole interactions as per the following relations.⁸⁷

$$E = E_0 + \Omega(W_{dd}) \quad (7)$$

Where E_0 is the energy of unperturbed levels and $\Omega(W_{dd})$ denote distribution of perturbations due to dipolar interactions with the medium. The W_{dd} is related with the mean dipole moments of chromophores and medium as per following relations.⁸⁷

$$W_{dd}^e \propto (\bar{\mu}_e \cdot \bar{\mu}_m) \quad (8)$$

$$W_{dd}^g \propto \bar{\mu}_g \cdot \bar{\mu}_m \quad (9)$$

For the edge excitation to occur, the W_{dd}^e should be maximum and W_{dd}^g should be minimum so that the dipolar interactions of the chromophores are minimum in the ground state and maximum in the excited state. It results in the photo selection of some chromophores with ground-state energy above E_g^{edge} and excited state energy below E_e^{edge} compared to the mean S_0 - S_1 excitations. In such a case the $\tau_R \gg \tau_F$ (Figure 4a).

Fluorescent imidazolium based NILs due to the segregation of polar/non-polar ensembles creates ground-state heterogeneity, with a local energetically distinct species having low 0-0 transition energy, moreover enhanced viscosity with the increase in chain length slow down the dielectric relaxation of other components around photo selected imidazolium causing the red-edge effect (Figure 4b).⁸⁸⁻⁸⁹ Moreover, these shifts become more prominent with an increase in the alkyl chain of the cation in neat IL ($[C_{2}mim][BF_4]$ ~ 280 nm; $[C_8mim][BF_4]$ ~ 390 nm).⁹⁰ While the red-edge spectroscopy is exploited to study the dynamics of proteins in an aqueous solution of various additives by excitation at the red-edge of the tryptophan absorbance,⁹¹ considering the widespread use of neat imidazolium or pyridinium ILs in biocatalysis,⁹² the red-edge effect of ILs⁹³ could be exploited as probe to understand the structure-function relation of enzymes upon cross-excitation at the red-edge of both tryptophan and neat ILs.

Besides inherent fluorescence, imidazolium cations have been chemically engineered with chiral emitters to display circularly polarized luminescence (CPL)⁹⁴⁻⁹⁵ for application as CPL emitter (Figure 4c) in electrochemical cells. The CPL is a phenomenon where the chiral chromophore with luminescence dissymmetry (g_{lum}) shows differential emission intensity of the right (I_R) or left (I_L) components of the circularly polarized light as per the following relations (Figure 5).⁹⁶

$$g_{lum} = 2 (I_L - I_R) / (I_L + I_R) \quad (10)$$

Besides being a CPL component, the NIL comprising tetrabutyl ammonium cation and chiral anions like proline, valinate, and aspartate were used to induce CPL in the achiral europium triflate salt via coordination of anions with the europium (Figure 5c).⁹⁷ Interestingly, the CPL spectra could be tuned according to the coordination of anions to Eu^{3+} highlighting the importance of customization.⁹⁷



Circularly Polarized Luminescence

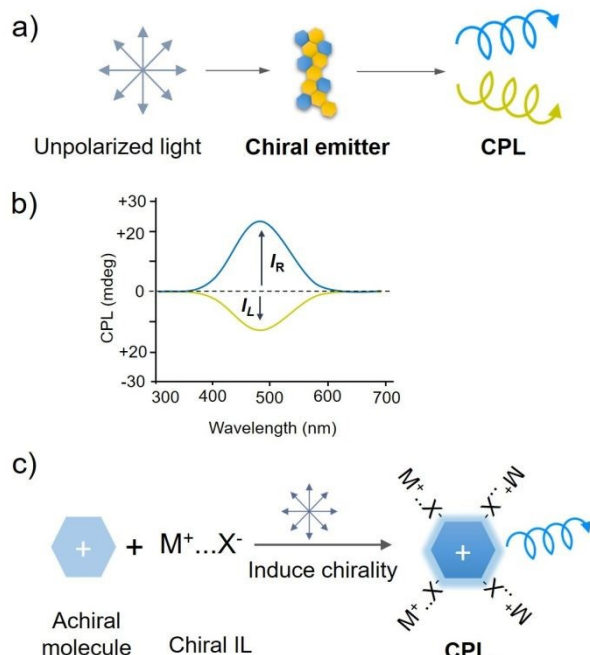


Figure 5. Illustration of the circularly polarized luminescence. a) Conversion of unpolarized light to the circularly polarized luminescent light by the chiral emitter, and b) CPL spectra showing differential emission of the left and right circularly polarized light. c) Induced CPL emission of an achiral compound upon mixing with a chiral ionic liquid.

Other than cations, anion customization has been also exploited to achieve suitably photoactive NILs. For instance, pairing of allyl-imidazolium cations of varying chain length with fluorescent $[\text{MnCl}_x\text{Br}_y]^{n-}$ anion resulted in phase change NILs with distinct thermochromic properties, which were exploited as sensors for temperature, relative humidity and alcohols by impregnating on the paper.⁹⁸ Kovalenko and coworkers paired photo-emissive lead halides anions with phosphonium cation as scintillators for application in fast neutron imaging with recoil proton detection, with high resolution and low γ -ray sensitivity (Figure 6).⁹⁹

Neutron Scintillation Imaging using NIL

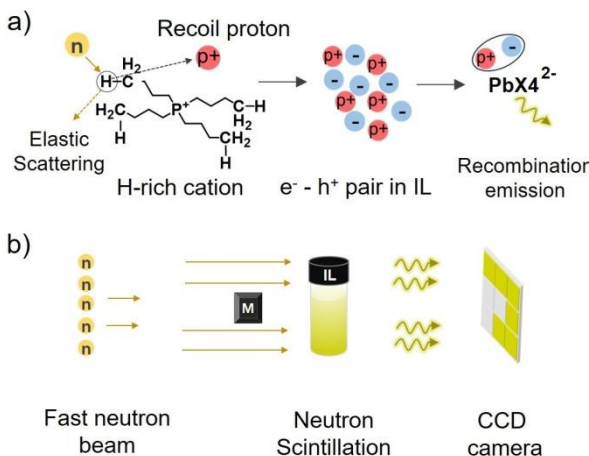


Figure 6. a) Illustration of the neutron scintillation by IL via generation of recoil proton after fast neutron bombardment, followed recombination emission through the formation of electron-hole pairs. b) Illustration of the neutron scintillation imaging using NIL as scintillator. Figure 6a, b adapted from ref 99 with CC-BY-NC-ND 4.0 open access

license from [American Chemical Society] [Kovalenko et al., ACS Photonics, 2021, 8, 3357–3364], copyright 2021. View Article Online DOI: 10.1039/D5CP04142B

Neutron scintillation is an optical process where neutrons interact with the material to produce tiny flashes of light, detected further by the photomultiplier tube. These NILs possess specific properties such as proton rich cation, narrow excitation, low scattering, high photoluminescence quantum yield and large stokes shift (1.7 eV) to avoid reabsorption desired for higher spatial resolution.⁹⁹ The H-rich cations of IL, generate recoil protons upon bombardment with fast neutrons, forming electron-hole pairs upon interaction with anions, which show high PL emission via charge recombination (Figure 6a).

Hisamoto and coworkers demonstrated Förster resonance energy transfer (FRET) in NIL, containing phosphonium cations, paired with sulfonated pyrene anion as donor (D), and lipophilic fluorescein anion as acceptor (A).¹⁰⁰

Förster Resonance Energy Transfer

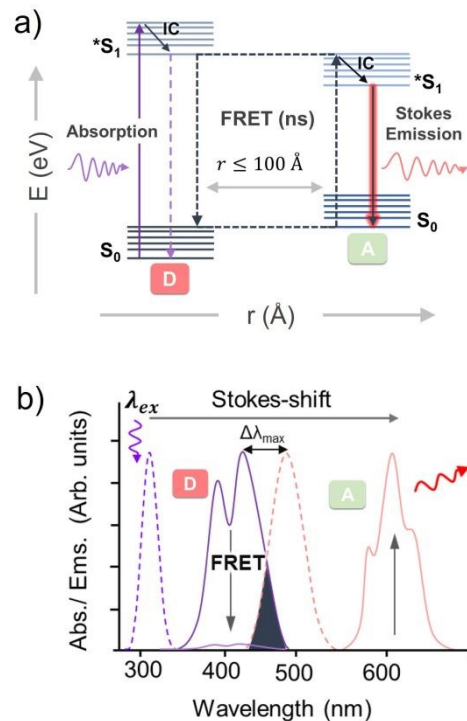


Figure 7. a) Illustration of the Förster resonance energy transfer through modified Jablonski diagram. The excited donor while coming back to the ground state transfers energy to the acceptor if found within 100 Å radius, resulting in the amplification of acceptor's emission at a longer wavelength. b) Illustration of the change in the absorption and emission spectra of donor and acceptor during FRET. IC = Internal conversion or vibrational relaxation.

FRET is a non-radiative energy transfer process that occurs via dipole-dipole interactions between the donor and acceptor molecules separated by <100 Å. As a result, the emission of the acceptor is increased at the expense of donor's emission due to FRET (Figure 7). The energy transfer efficiency (E) in FRET can be estimated using the following relation.²⁸

$$E = R_0^6 / (R_0^6 + r^6) \quad (11)$$

Where r is the distance between the donor and acceptor and R_0 is the Förster distance which signifies 50% energy transfer efficiency.

The FRET in the NIL mixture was utilized to form solvent doped-PVC membrane with improved ion extraction-based sensing.¹⁰⁰ The liquid nature of the IL played a key role here for supporting the molecular diffusion of anionic chromophores (donor and acceptor), in the trapped FRET liquid for efficient energy transfer.

Kimizuka and co-workers demonstrated Dexter energy transfer (DET) in NIL comprising tetra-alkyl phosphonium cations and photoactive anions such as sulfonated anthracene and 4-(2-phenyloxazol-5-yl)benzene for green to blue, and blue to UV photon upconversion via triplet-triplet annihilation photon upconversion (TTA-UC)¹⁰¹⁻¹⁰³ (Figure 8).

Dexter Energy Transfer in TTA-UC

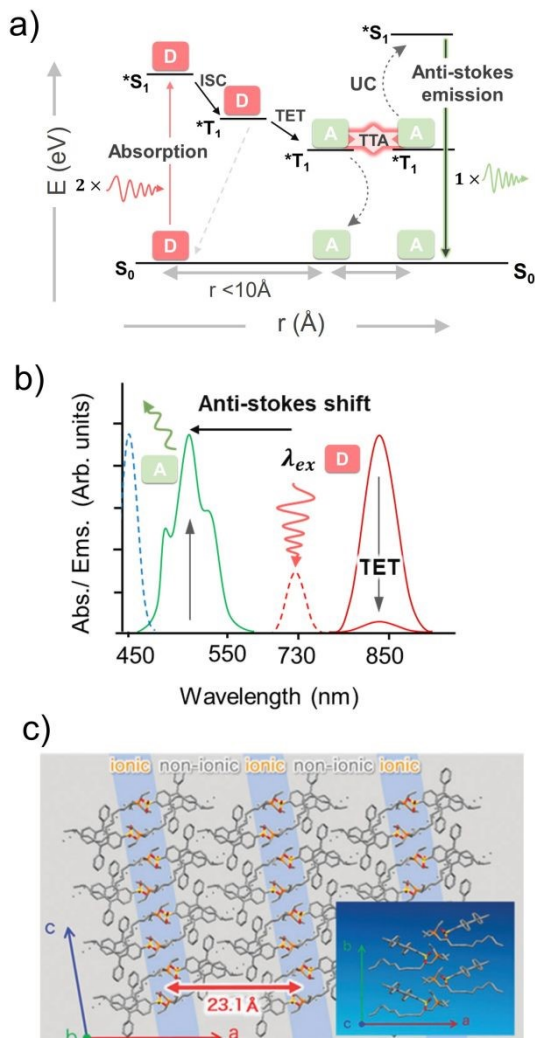


Figure 8. a) Illustration of the sequential energy transfer in TTA-UC. The sensitizer/donor upon absorption of low energy photon goes to the triplet-state via intersystem crossing (ISC), followed by the r triplet energy transfer to the annihilator (TET), which undergoes triplet-triplet annihilation (TTA), leading to the formation of an excited singlet-state of the annihilator, which show the anti-stokes delayed emission. b) Illustration of the change in emission spectra of photosensitizer and annihilator during TTA-UC. c) Crystal structure of ionic crystals of $[C_{24}(C_2)_3P]^+[DPASO_4^-]$ viewed along the b-axis, showing a lamellar structure consisting of ionic and non-ionic layers. Inset: the structure viewed along the c-axis to see a long tail alkyl chain sandwiched between two anthracene rings. Figure 8c has been reproduced from ref 102 with permission from [The Royal Society of Chemistry, London] [Kimizuka *et al.*, *Phys. Chem. Chem. Phys.*, 2018, 20, 3233-3240], copyright 2018.

TTA-UC is a non-linear optical process that occurs in the annihilator's ensembles doped with a triplet photosensitizer in the oxygen free conditions. The photosensitizer upon excitation at low energy undergo intersystem to the triplet-state and while coming back to the ground-state sensitize the annihilator triplets via triplet-triplet energy transfer. The sensitized annihilator triplets then undergo annihilation via spin-exchange coupling, resulting in the formation of an emissive singlet-state of the annihilator which show upconversion emission (Figure 8a). The probability of singlet formation (f) can be estimated using the following relation.¹⁰¹

$$f = 2 \times \Phi_{UC} / \Phi_{isc} \cdot \Phi_{TET} \cdot \Phi_{TTA} \cdot \Phi_F \quad (12)$$

Where Φ_{UC} , Φ_{isc} , Φ_{TET} , Φ_{TTA} , and Φ_F are quantum yields of upconversion, intersystem crossing of the photosensitizer, triplet energy transfer from the photosensitizer to the annihilator, triplet-triplet annihilation and fluorescence quantum yield of the annihilator.

The high viscosity of NILs play a key role in TTA-UC as it decreases the oxygen diffusion which protect chromophores triplets oriented between non-polar domains of the IL, from quenching by the ground state triplet oxygen in aerated conditions (Figure 8c).¹⁰¹⁻¹⁰³ Moreover, the confinement of annihilators in contiguous ionic arrays allow effective triplet-energy transfer for an efficient energy upconversion.¹⁰⁴

The customized nature of ILs has been exploited to generate laser pulses either in the bulk or confined liquid domain.¹⁰⁵⁻¹⁰⁸ In an interesting report Kupfer and coworkers utilized the vibrational energy in the chemical bonds of NIL, ethyl-3-methylimidazolium dicyanamide ($[C_2mim][dca]$) to generate nanosecond mid infra-red orange radiation (603 nm) by down-conversion of 532-nm laser pulses via molecular stimulated Raman scattering (SRS) (Figure 9).¹⁰⁵

SRS in NIL to generate nanosecond laser pulse

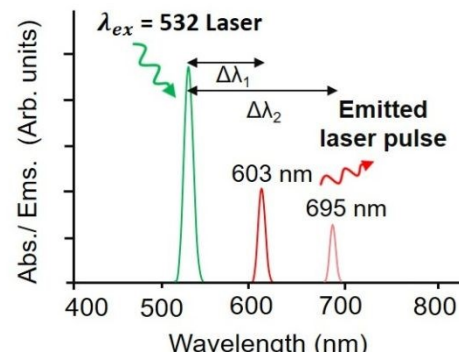


Figure 9. Illustration of the spectral changes during photon downconversion of 532 nm laser pulse due to Stimulated Raman Scattering in an IL ($[C_2mim][dca]$ with Raman active dicyanamide anion). Figure 9 adapted from ref 105 with permission from [American Physical Society] [Palmer *et al.*, *Phys. Rev. Appl.*, 2023, 19, 014052], copyright 2023.

SRS is a non-linear optical phenomenon that involve the inelastic scattering of photons from a coherently excited state of the Raman active material.

Consequently, the pump wavelength is transformed into Stokes and anti-Stokes wavelengths, which are shifted by the dominant bond vibrational frequency. The Raman frequency shift in SRS can be estimated using the following relation.¹⁰⁵

ARTICLE

Journal Name

$$\omega_R = \omega_L \pm N_R \omega_v \quad (13)$$

Where ω_R , ω_L , and ω_v are frequencies of the Raman shift, pump, and bond vibration, and N_R is the shift order in case of cascade process.

In the ethyl-3-methylimidazolium dicyanamide, the down converted emission corresponds to a Raman shift of 2200 cm^{-1} due to dominant bond vibration of dicyanamide anion at this frequency.¹⁰⁵

Besides ethyl-3-methylimidazolium dicyanamide, molecular SRS was also observed with other NILs, comprising bis(trifluoromethylsulfonyl)amide anion paired with 1-butyl-1-methylpyrrolidinium and butylpyridinium cation for downconverting the 532 nm laser pulse to 578 nm , 599 and 632 nm via SRS.¹⁰⁵ Further customization of the NIL structure with a suitable Raman active cation or anion can also lead to SRS based energy upconversion to produce high frequency pulses with lifetimes varying between nano to femtoseconds.¹⁰⁵

Sun and coworker used the NIL, 1-butyl-3-methyl imidazolium hexafluorophosphate as a gain medium to develop microfluidic ionic liquid dye laser using BODIPY as dye operating via whispering gallery modes (WGMs) based lasing emission.¹⁰⁶ WGM is an optical phenomenon generally observed in micro-sized circular resonators due to the circulation of light via total internal reflection along the curved boundary, resulting in the formation of resonance patterns.¹⁰⁷⁻¹⁰⁸ The microdroplets of 1-butyl-3-methyl imidazolium hexafluorophosphate doped with BODIPY when pumped with 485 nm pulsed laser above lasing threshold $40.1\text{ }\mu\text{J/mm}^2$ showed WGMs based lasing emission at 527 nm different from the normal fluorescence emission of BODIPY.¹⁰⁶ The refractive index and viscosity of the used IL played a key role to form droplets with optically smooth surfaces to avoid losses due to scattering during lasing.

NIL, Deng and coworker reported electro-optical modulation by hydrophobic NILs, in the NIR region ($\lambda = 1330$ or 1530 nm) under the application of a strong electric field ($E = \pm 4V$) due to N-H or C-H vibration and their overtone and combination transitions leading to radiationless deactivation or absorption in a microfluidic device.¹⁰⁹ electro-optical modulation amplitude increase due to the change in carrier concentration near the electrodes with an increase in the electrical conductivity of ILs.

Borra and coworkers exploited the higher reflectance in the infra-red region, low vapour pressure under vacuum, and low freezing temperature~ 175 K of silver coated NIL, 1-Ethyl-3-methyl imidazolium ethylsulfate, to be used as liquid mirror in infra-red lunar telescope.¹¹⁰ The reflectance (R) is an optical property of the material indicating the fraction of light reflected in comparison to the transmitted light. The R depends on the angle of incidence (θ) and polarization of light (P), and refractive index (n) of the medium. The R of a liquid at $\theta = 0^\circ$ can be calculated using the Fresnel equation.¹¹¹

$$R = \left(n_1 - n_2 \mid n_1 + n_2 \right)^2 \quad (14)$$

Where n_1 and n_2 are refractive index of air and liquid under study. The value of R varies between 0 to 1. However, the equation can change according to the change in the polarization and angle of incidence of the light.

Besides reflectance, the liquidity and surface tension¹¹² of NILs leverage advantage of shape change to create¹¹³ mirrors with high parabolic surfaces in microgravity. While it was considered a great breakthrough at that time, no further development related to this were reported in the open literature until a recent internship report by Szoboly et al.¹¹³ The team conducted the work at NASA Goddard Space Flight Center to develop self-healing silver nanoparticles coated NILs mirrors for next generation of liquid space telescopes.¹¹³ This is an exciting, but a highly underexplored area in NIL research with direct application in space exploration telescope.¹¹⁴⁻¹¹⁵ A representative images showing reflection of NIR light by IL coated silver nanoparticles is shown as Figure 10.



Figure 10. Illustration of the infra-red reflectivity of silver and chromium coated ionic liquid droplets. The reflectivity increases in the infra-red in the presence of ionic liquids compared to PEG, which can be used liquid mirror in telescope. This image is drawn using the free ChatGPT AI [January 13, 2026].

Due to their nano-heterogeneous structure and polarizability NILs can diffract the light of a specific wavelength corresponding the dimension of nano-heterogeneity.¹¹⁶ This property makes the NILs as useful additive to increase the diffraction efficiency, resolution, and sensitivity of photopolymerizable hologram materials (Figure 11).¹¹⁷⁻¹¹⁸ Moreover customization of their viscosity makes them suitable diffusing solvents during photopolymerization.¹¹⁷⁻¹¹⁸

NIL as efficient diffractor for Holograms

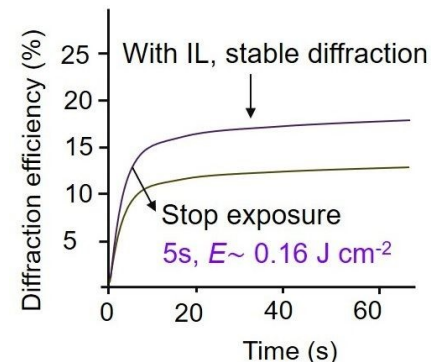


Figure 11. Figure showing improved diffraction efficiency of photopolymerizable material with the addition of ionic liquid. Figure 11 has been adapted from ref 117 with permission from [AIP Publishing] [Veith et al. *Appl. Phys. Lett.*, 2008, 93, 141101], copyright 2008

Neat Deep Eutectic Solvents as Photonic Component



Similar to ILs, the customized nature of DESs can be exploited to develop photo responsive DESs by substitution of one of the components with a photoactive molecule. Neat DESs (NDESs) are considered next generation green solvents as replacement for ILs due to similarity in their physical properties.^{20,27} However, unlike NILs, NDESs have been less explored in photonics which gives an opportunity to develop this field. The refractive index (linear or non-linear) is among the most significant optical properties of DESs which leverage their potential applications as medium for liquid-based optical communications.¹¹⁹⁻¹²¹ The non-linear refractive index (n_2) varies with the light intensity (I) as per the following equation 15.¹²¹

$$n - n_0 = \Delta n = n_2 I \quad (15)$$

Further it is related to the third order non-linear susceptibility ($\chi^{(3)}$) as per equation 16.¹²¹

$$n_2 = \frac{3\chi^{(3)}}{4\epsilon_0 c n^2} \quad (16)$$

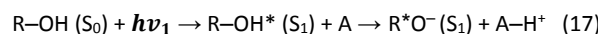
Where ϵ_0 relative permittivity of free space and c is the velocity of light. Experimentally it can be measured using Z-scan technique.¹²² Some DESs such as [Cho]Cl: lactic acid, show negative third order non-linear refractive index which can support bright optical solitons over long distances to improve the performance of long-distance optical communication.¹²¹ This is due to the structural heterogeneity of DESs that creates localized structural domains smaller than the wavelength of excitation light. The negative non-linear refractive index arises due to the thermal lensing effect¹²³ caused by heating of the excitation spot by high energy laser pulse than the edges, thus creating a refractive index gradient due the temperature gradient caused by the localized heating. Interestingly, the customized nature leverage tuning of the magnitude of negative non-linear refractive index of DESs by changing the ratio and structure of HBD and HBA. Considering the available HBA or HBD, and their customized nature, thousands of DESs, supporting bright optical soliton can be synthesized for enhance optical communication.

Gupta and coworkers developed a fluorescent NDESs (Heptyltriphenylphosphine (M^+), bromide (X^-), and decanoic acid (zY)) which was used as sensor to detect D_2O via increase in fluorescence intensity.¹²⁴ Hopkins and coworkers exploited customized nature of DESs to synthesize chiral DESs comprising alkylammonium chloride salts as HBA and chiral HBD (amino acids, organic acids and monosaccharide) to leverage CPL property to a racemic mixture of luminescent dissymmetric lanthanide complexes.¹²⁵⁻¹²⁶ Further changing the HBA with alkylphosphonium chloride, enhanced the enthalpy and entropy of chiral discrimination by 50%, demonstrating advantage of the customized nature of DESs.¹²⁷

Murakami and co-workers exploited thermal stability of DESs as solvents to host organic chromophores (PtOEP, PdOEP and DPA) to achieve high efficiency upconversion of green photons to blue photons.¹²⁸ Unlike ILs based TTA-UC system where chromophores were part of the IL structure,¹⁰¹⁻¹⁰⁴ DESs have been used just as native solvents. However, advancements can be made in this direction by introducing HBD property to the TTA-UC chromophores to develop solvent free TTA-UC DESs.

The dynamic heterogeneity, hydrogen bond acidity or basicity of NDESs has also been exploited to study excited state proton-transfer

(ESPT) operating at the nanosecond timescale using either pyranine or naphthol's as proton-transfer probes.¹²⁹⁻¹³⁰ DOI: 10.1039/CSPD04142A
ESPT can be understood using following equations.¹³¹



Where $R-OH$, and A represents the proton donor and acceptor. The deprotonated molecule in the excited singlet state (S_1) can relax to the ground state via radiative ($h\nu_2$) or vibrational relaxation via non-radiative (**heat**) emission. Since ESPT involve proton transfer, the DESs comprising of HBD and HBA can directly participate in the process.¹²⁹ Guchhait and coworkers also exploited the dynamic heterogeneity of DESs and reported ESPT at the nanosecond timescale (2.6 to 7.5 ns) using pyranine as proton donor in the DESs, $[(C_2)_4N]^+[Br]^-:(CH_2OH)_2$, $[(C_2)_4N]^+[Br]^-:$ Glycine, $[(C_2)_4N]^+[Cl]^-:(CH_2OH)_2$, $[Cho]^+[Cl]^-:(CH_2OH)_2$ confined inside the supported liquid membrane due to long-range interfacial order effects. The long-range interfacial order in the confined domain was confirmed from slow dynamics of solvent relaxation and red-edge effect.¹³⁰

Conclusions

The customized nature of NILs by large, and NDESs to some extent, has been exploited for chemical engineering of their structure for a specific linear or non-linear optical application. These processes include red-edge effect, circularly polarized luminescence, neutron scintillation, photon conversion via FRET, DET, stimulated Raman scattering, electro-optical modulation, micro-fluidic dye lasers, reflector for liquid mirrors, directors in holograms, and refractors for liquid-based optical communication and medium for ESPT. However, these studies are limited to proof-of-concept level, though with potential applications discussed in the respective section. Other than the photonic part, properties like viscosity, polarity, and refractive index, broad thermal range, structural heterogeneity, conductivity, large electrochromic window and hydrogen bond acidity or basicity play a key role in their successful implementation in the reported photonic systems as summarized in Table 1. Upon evaluation of the use of NDESs in comparison to NILs within photonic systems, it becomes evident that NDESs are still in the early stages of development, despite sharing numerous physicochemical characteristics with NILs. They are regarded as an advanced version of NILs primarily due to their environmental sustainability, which is attributed to their low toxicity, biodegradability, and low-cost synthesis.¹³² While these attributes may provide NDESs with certain advantages over NILs in certain applications, the requirements for many photonic applications necessitate photoactive materials that exhibit excellent photostability along with broad absorption and emission ranges. Consequently, one of the essential components



ARTICLE

Journal Name

must include either a polycyclic aromatic hydrocarbon (which is typically considered toxic), metals,¹³³ semiconductor nanoparticles,¹³⁴⁻¹³⁵ or a perovskite compounds (may use toxic metals like Pb, Cd)¹³⁶⁻¹³⁷ and carbon nanoparticles.¹³⁸⁻¹³⁹ NIL also offers great structural versatility to design photoactive ionic liquids with a vast number of polycyclic aromatic organic cations or anions because of its two-component nature. Whereas the structural complexity of DESs due to the multicomponent nature held together by hydrogen bonding, limits its versatility beyond bio-derived components. Therefore, currently NILs are leading the photonic applications in the neat form compared to NDESs. However, the sustainable nature of DESs holds high value compared to NILs when considered only as solvents to disperse photoactive compounds to study various optical processes,^{128,130-131} followed by easy separation at the end-of-life. For consideration purely as photonic component more NDESs with polycyclic aromatic dyes as one of the components need to be synthesized for a valid comparison with NILs in photonic applications.

What Next for NILs and DESs in Photonics?

The thermal stability is among the key properties of NILs and DESs to be exploited in photonics, as it can address the heating effects during light-matter interaction.¹⁴⁰⁻¹⁴³ Heating can negatively alter the optical properties, such as resonance frequencies, and signal integrity due to the thermal cross-talk and change in refractive index to affect the device performance.¹⁴⁴ However, the higher heat capacities of NILs and DESs can serve as a heat sink in case of thermo-optical effects. The studies on photonics in liquid-state (chemical or metallic liquids) are slowly gaining momentum.¹⁴⁵⁻¹⁴⁶ NILs and DESs can contribute immensely as an organic liquid to this, with the customized nature of their thermophysical and chemical properties. For example, liquid water, due to its absorption in tetra-hertz range, generates a broadband terahertz wave,¹⁴⁵⁻¹⁴⁶ and high plasma frequency of Gallium liquid has been exploited to realize UV plasmonic structures.¹⁴⁷ Moreover, the absence of domain boundaries and the smoothness of surfaces in liquid metal nanostructures result in an extended carrier relaxation time, consequently leading to reduced losses for surface plasmons in addition to broad thermal ranges.¹⁴⁸ On similar lines, NILs, and DESs can be explored as liquid organic/inorganic semiconductors¹⁴⁹⁻¹⁵⁰ by synthesizing the variants comprising polycyclic aromatic hydrocarbons and liquid metal salts. While a few proof-of-concept studies, especially on NILs, have been already reported in this direction,¹⁰³⁻¹⁰⁴ broadening the scope of detailed fundamental investigations related to applicable photonics can further attract the attention of the scientific community in this direction. For instance, the feasible advancement of liquid-junction solar cells¹⁵¹ or liquid solar cells¹⁵² as a sustainable clean energy alternative could significantly enhance the use of NIL or DESs-based liquid organic semiconductors as *in situ* photon converters^{103-104, 153-154} or solar concentrators¹⁵⁵⁻¹⁵⁶ to capture light either below or above the solar cell's band gap, thereby improving performance.¹⁵⁵⁻¹⁵⁸ While both NILs and DESs have been used as electrolyte or redox mediator in dye sensitized solar cells (DSSCs)¹⁵⁹⁻¹⁶¹ due to their conductivity and non-volatility, using as dye, electrolyte and redox mediator in a single system would be an ideal advancement in this direction. For example, anthracene-based dyes have been used as dye and photon upconverter in DSSCs,¹⁵⁷ hence

suitable NDESs and NILs comprising redox active dyes, if synthesized can serve both as sensitizer dye, photon converter,¹⁶² and redox mediator in DSSCs. Both NILs and NDESs possess suitable properties for applications in liquid luminescent solar concentrators.¹⁶² For example, high refractive index, heterogenous structure, differential polarity to solubilize luminophores and more importantly structural tunability to design liquids containing luminophores with high Stokes-shifts and thermal stability. Despite having suitable properties NILs¹⁶³⁻¹⁶⁴ or DESs have been rarely investigated for LSCs. With the emergence of liquid based LSCs, both NILs and NDESs could turn out to be a promising future candidate for LSCs if suitable design principles considering photostability of luminophores are envisioned. Owing to their thermochemical phase change characteristics, both NILs and DESs possess significant potential as materials for thermal energy storage.¹⁶⁵⁻¹⁶⁷ Molecular solar thermal energy storage systems (MOST) are emerging as clean energy alternatives where solar energy is stored as heat in molecular photoswitches.¹⁶⁸⁻¹⁷⁰ Besides fundamental research, recent years have seen a lot of reports on the development of MOST devices,¹⁶⁷⁻¹⁷¹ where photoswitches have been dissolved in organic solvents (generally toxic), were tested at different flow-rates, and residence-times to absorb maximum solar photons to be stored as heat by the photisomer.¹⁷² A typical example of MOST is Norbornadiene (NBD)↔ Quadricyclane (QC) system, where NBD, after absorbing UV photons, gets converted to QC form, which stores the heat as high as 93 kJ mol⁻¹.¹⁶⁹ Besides NBD, several other organic photoswitches like azobenzene, azopyrazole, dihydroazulene, and orthodianthrylbenzenes are emerging as suitable solar-thermal energy storage materials.^{169,173} As a green alternative to organic solvents, mixtures of water and non-ionic surfactants have been explored at high NBD concentrations, generally needed to store higher energy.¹⁷⁴ However, water-surfactant mixtures are prone to phase separation above a certain concentration of the photoswitch or surfactant due to the solubility limitations. NILs or NDESs can overcome the solubility limitations as the photoswitches can be transformed directly into thermally stable NILs or DESs with required viscosities and vapor pressure through appropriate chemical engineering. This transformation can lead to improved heat storage capabilities, as it combines the heat storage resulting from the phase change in NILs or DESs with the heat absorbed from solar photons by the photoswitches.

Author contributions

P. B. conceived the idea of this perspective article, wrote the first draft and revised manuscript. M.M. assisted in editing of the manuscript.

Conflicts of interest

"There are no conflicts to declare"

Data availability



There is no data to be declared. The Supplementary information Table S1, contains full names of the abbreviations used in this manuscript.

Acknowledgements

P.B. acknowledges Ramón y Cajal grant from Spanish State Investigation Agency (Grant no. J03416), and La-Caixa junior research leadership-post doctoral project PHOLCEB (ID: 100010434, fellowship code: LCF/BQ/P122/11910023) for financial support. M. M. and P. B. acknowledge the State Investigation Agency, through the Severo Ochoa Programme for Centres of Excellence in R&D (CEX2023-001263-S) and project PID2021-123873NB-I00 for financial support. Some parts of the TOC graphic image and Figure 9 have been drawn using free drawing tool at Chatgpt.com.

Notes and references

- 1 S. P. M. Ventura, F. A. Silva, M. V. Quental, D. Mondal, M. G. Freire, J. A. P. Coutinho, *Sep. Sci.*, 2016, **39**, 3505-3520.
- 2 P. Bharmoria, A. A. Tietze, D. Mondal, T. S. Kang, A. Kumar, M. G. Freire, *Chem. Rev.*, 2024, **124**, 3037-3084.
- 3 N. Yadav, P. Venkatesu, *Phys. Chem. Chem. Phys.*, 2022, **24**, 13474-13509.
- 4 A. Sanchez-Fernandez, J. H. Nicholson, S. M. M. Huaman, C. A. Romero, J.-F. Poon, S. Prevost, A. P. S. Brogan, *Commun. Chem.*, 2025, **8**, 173.
- 5 T. Zhou, C. Gui, L. Sun, Y. Hu, H. Lyu, Z. Wang, Z. Song, G. Yu, *Chem. Rev.*, 2023, **123**, 12170-12253.
- 6 S. Chattopadhyay, S. Kataria, S. Prusty, M. Subban, A. Kumar, S. Sutradhar, *ACS Symposium Series*, 2025, **1504**, 135-153.
- 7 R. M. Moshikur, M. R. Chowdhury, M. Moniruzzaman, M. Goto, *Green Chem.*, 2020, **22**, 8116-8139.
- 8 E. Chevé-Kools, Y. H. Choi, C. Roullier, G. Ruprich-Robert, R. Grougnet, F. Chapelard-Leclerc, F. Hollmann, *Green Chem.*, 2025, **27**, 8360-8385.
- 9 Q. Hou, X. Qi, M. Zhen, H. Qian, Y. Nie, C. Bai, S. Zhang, X. Baia, M. Ju, *Green Chem.*, 2021, **23**, 119-231.
- 10 Y. Gu, F. Jérôme, *Chem. Soc. Rev.*, 2013, **42**, 9550-9570.
- 11 P. Bharmoria, M. J. Mehta, I. Pancha, A. Kumar, *J. Phys. Chem. B* 2014, **118**, **33**, 9890-9899.
- 12 E. L. Smith, A. P. Abbott, K. S. Ryder, *Chem. Rev.*, 2014, **114**, 11060-11082.
- 13 D. R. MacFarlane, M. Forsyth, P. C. Howlett, J. M. Pringle, J. Sun, G. Annat, W. Neil, E. I. Izgorodina, *Acc. Chem. Res.*, 2007, **40**, 1165-1173.
- 14 Z. Liu, F. Feng, W. Feng, G. Wang, B. Qi, M. Gong, F. Zhang, H. Pang, *Energy Environ. Sci.*, 2025, **18**, 3568-3613.
- 15 S. Zhang, N. Sun, X. He, X. Lu, X. Zhang, *J. Phys. Chem. Ref. Data*, 2006, **35**, 1475-1517.
- 16 D. Yu, Z. Xue, T. Mu, *Chem. Soc. Rev.*, 2021, **50**, 8596-8638.
- 17 K. Fumino, S. Reimanna, R. Ludwig, *Phys. Chem. Chem. Phys.*, 2014, **16**, 21903-21929
- 18 L. J. B. M. Kollau, M. Vis, A. van den Bruinhorst, A. C. C. Esteves, R. Tuinier, *Chem. Commun.*, 2018, **54**, 13351-13354
- 19 H. Zhang, J. M. Vicent-Luna, S. Tao, S. Calero, R. J. J. Riobóo, M. L. Ferrer, F. del Monte, M. C. Gutiérrez, *ACS Sustainable Chem. Eng.*, 2022, **10**, 1232-1245
- 20 R. Hayes, G. G. Warr, R. Atkin, *Chem. Rev.*, 2015, **115**, 6357-6426
- 21 D. Lengvinaitė, S. Kvedaraviciute, S. Bielskutė, V. Klimavicius, V. Balevicius, F. Mocci, A. Laaksonen, K. Aidas, *J. Phys. Chem. B*, 2021, **125**, 3255-3266
- 22 María J. Dávila, S. Aparicio, R. Alcalde, B. García, J. M. Leal, *Green Chem.*, 2007, **9**, 221-232 [View Article Online](#) DOI: 10.1039/D5CP0412B
- 23 A. A.-Bodour, N. Alomari, G. P.-Duran, S. Rozas, G. I.-Silva, S. Aparicio, A. G.-Vega, M. Atilhan, *Energy Fuels* 2025, **39**, 12791-12829
- 24 Z. Lei, B. Chen, Y.-M. Koo, D. R. MacFarlane, *Chem. Rev.*, 2017, **117**, 6633-6635.
- 25 B. B. Hansen, S. Spittle, B. Chen, D. Poe, Y. Zhang, J. M. Klein, A. Horton, L. Adhikari, T. Zelovich, B. W. Doherty, B. Gurkan, E. J. Maginn, A. Ragauskas, M. Dadmun, T. A. Zawodzinski, G. A. Baker, M. E. Tuckerman, R. F. Savinell, J. R. Sangoro, *Chem. Rev.*, 2021, **121**, 1232-1285.
- 26 J. A. Sirviö, M. Visanko, H. Liimatainen, *Green Chem.*, 2015, **17**, 3401-3406.
- 27 V. Pandey, T. Pandey, R. S. Kaundal, *Deep Eutectic Solvents ACS Symposium Series* 2025, **1504**, Chapter 3, 77-95.
- 28 P. Bharmoria, S.P.M. Ventura (2019). *Optical Applications of Nanomaterials*. In: A. Bhat, I. Khan, M. Jawaid, F. Suliman, H. Al-Lawati, S. Al-Kindy, (eds) nanomaterials for healthcare, energy, and environment. Advanced structured materials, vol 118. Springer, Singapore.
- 29 <https://www.chem.uci.edu/~potma/lecture3.pdf>
- 30 G. Agrawal, Nonlinear fiber optics, fifth edn. Chapter 1. Elsevier Inc., 2013, pp 1-25.
- 31 S. L. Bondarev, V. N. Knyuksho, S. A. Tikhomirov, *J. Appl. Spectrosc.*, 2002, **69**, 230-237.
- 32 Transition moment in IUPAC Compendium of Chemical Terminology, 5th ed. International Union of Pure and Applied Chemistry; 2025.
- 33 R. Hayes, G. G. Warr, R. Atkin, *Chem. Rev.* 2015, **115**, 6357-6426
- 34 M. Sha, Y. Liu, H. Dong, F. Luo, F. Jiang, Z. Tang, G. Zhu, G. Wu, *Soft Matter*, 2016, **12**, 8942-8949.
- 35 Y.-L. Wang, B. Li, S. Sarman, F. Mocci, Z.-Y. Lu, J. Yuan, A. Laaksonen, M. D. Fayer, *Chem. Rev.*, 2020, **120**, 5798-5877
- 36 Y. Ji, R. Shi, Y. Wang, G. Saielli, *J. Phys. Chem. B*, 2013, **117**, 1104-1109
- 37 M. Torkzadeh, M. Moosavi, *J. Phys. Chem. B*, 2020, **124**, 11446-11462
- 38 Z. Hu, C. J. Margulis, *PNAS*, 2006, **103**, 831-836.
- 39 V. H. Paschoal, L. F. O. Faria, M. C. C. Ribeiro, *Chem. Rev.*, 2017, **117**, 7053-7112.
- 40 T. Frömbgen, K. Drysch, T. Tassaing, T. Buffeteau, O. Hollóczki, B. Kirchner, *Angew. Chem. Int. J.*, 2025, **64**, e202502885.
- 41 P. Oulevey, S. Luber, B. Varnholt, T. Bürgi, *Angew. Chem. Int. J.*, **2016**, **55**, 11787-11790.
- 42 A. Marini, A. M.-Losa, A. Biancardi, B. Mennucci, *J. Phys. Chem. B*, 2010, **114**, 17128-17135.
- 43 S. Spittle, D. Poe, B. Doherty, C. Kolodziej, L. Heroux, M. A. Haque, H. Squire, T. Cosby, Y. Zhang, C. Fraenza, S. Bhattacharyya, M. Tyagi, J. Peng, R. A. Elgammal, T. Zawodzinski, M. Tuckerman, S. Greenbaum, B. Gurkan, C. Burda, M. Dadmun, E. J. M. Joshua Sangoro, *Nat. Commun.*, 2022, **13**, 219
- 44 M. N. Kamar, A. Mozhdehei, B. Dupont, R. Lefort, A. Moréac, J. Ollivier, M. Appel, D. Morineau, *J. Chem. Phys.*, 2025, **163**, 134506.
- 45 A. Malik, and H. K. Kashyap, *Phys. Chem. Chem. Phys.*, 2023, **5**, 19693-19705
- 46 T. Rinesh, H. Srinivasan, V. K. Sharma, V. García Sakai, S. Mitra, *J. Chem. Phys.*, 2025, **162**, 244503.
- 47 R. K. Venkatraman, A. J. Orr-Ewing, *Acc. Chem. Res.*, 2021, **54**, 4383-4394.
- 48 X. Wang, S. Zhang, J. Yao, H. Li, *Ind. Eng. Chem. Res.*, 2019, **58**, 7352-7361
- 49 M. A. Ab Rani, A. Brant, L. Crowhurst, A. Dolan, M. Lui, N. H. Hassan, J. P. Hallett, P. A. Hunt, H. Niedermeyer, J. M. Perez-



ARTICLE

Journal Name

Arlandis, M. Schrems, T. Welton, and R. Wilding, *Phys. Chem. Chem. Phys.*, 2011, **13**, 16831–16840.

50 Ashish Pandey, Rewa Rai, Mahi Pala and Siddharth Pandey, *Phys. Chem. Chem. Phys.*, 2014, **16**, 1559–1568.

51 Y.-D. Song, Q. T. Wang, L. Chen, *J. Phys. Org. Chem.*, 2023, **36**, e4474.

52 R. K. Venkatraman, A. J. Orr-Ewing, *Acc. Chem. Res.*, 2021, **54**, 4383–4394.

53 Q. Zhou, M. Zhou, Y. Wei, X. Zhou, S. Liu, S. Zhang, B. Zhang, *Phys. Chem. Chem. Phys.*, 2017, **19**, 1516–1525.

54 J. Mei, N. L. C. Leung, R. T. K. Kwok, J. W. Y. Lam, B. Z. Tang, *Chem. Rev.*, 2015, **115**, 11718–11940.

55 S. Suzuki, S. Sasaki, A. S. Sairi, R. Iwai, B. Z. Tang, G. Konishi, *Angew. Chem. Int. J.*, 2020, **59**, 9856–9867.

56 C. Gao, L. Fu, J. Wang, Y. Chu, L. Gao, H. Qiu, J. Chen, *Chem. & Biomed. Imag.* 2025, **3**, 837–848.

57 A. Banerjee, K. De, U. Bhattacharjee, *J. Phys. Chem. B*, 2024, **128**, 849–856.

58 C. R. Benson, L. Kacenauskaitė, K. L. VanDenburgh, W. Zhao, B. Qiao, T. Sadhukhan, M. Pink, J. Chen, S. Borgi, C.-H. Chen, B. J. Davis, Y. C. Simon, K. Raghavachari, B. W. Laursen, A. H. Flood, *Chem.*, 2020, **6**, 1978–1997.

59 X. Ma, R. Sun, J. Cheng, J. Liu, F. Gou, H. Xiang, X. Zhou, *J. Chem. Educ.*, 2016, **93**, 345–350.

60 Y. Huang, J. Xing, Q. Gong, L.-C. Chen, G. Liu, C. Yao, Z. Wang, H.-L. Zhang, Z. Chen, Q. Zhang, *Nat. Commun.*, 2019, **10**, 169.

61 J. T. Edward, *J. Chem. Educ.*, 1970, **47**, 261.

62 Chen Ye Victor Gray, Jerker Mårtensson, Karl Börjesson, *J. Am. Chem. Soc.*, 2019, **141**, 9578–9584.

63 A. A. Veldhorst, M. C. C. Ribeiro, *J. Chem. Phys.*, 2018, **148**, 193803.

64 Y. L. Wang, B. Li, S. Sarman, F. Mocci, Z.-Y. Lu, J. Yuan, A. Laaksonen, M. D. Fayer, *Chem. Rev.*, 2020, **120**, 798–5877.

65 R. Clark, M. A. Nawawi, A. Dobre, D. Pugh, Q. Liu, A. P. Ivanov, A. J. P. White, J. B. Edel, M. K. Kuimova, A. J. S. McIntosh, T. Welton, *Chem. Sci.*, 2020, **11**, 6121–6133.

66 S. Chatterjee, S. H. Deshmukh, S. Bagchi, *J. Phys. Chem. B*, 2022, **126**, 8331–8337.

67 L. Naimovičius, M. Dapkevičius, E. Radiunas, M. Miroshnichenko, G. Kreiza, C. Alcaide, P. Baronas, Y. Sasaki, N. Yanai, N. Kimizuka, A. B. Pun, M. Solà, P. Bharmoria, K. Kazlauskas, K. Moth-Poulsen, *Chem. Sci.*, 2025, **16**, 20255–20264.

68 H. Kouno, Y. Sasaki, N. Yanai, N. Kimizuka, *Chem. Eur. J.*, 2019, **25**, 6042.

69 P. Bharmoria, S. Hisamitsu, H. Nagatomi, T. Ogawa, M.-a. Morikawa, N. Yanai, N. Kimizuka, *J Am. Chem. Soc.*, 2018, **34**, 10848–10855.

70 P. Bharmoria, S. Hisamitsu, Y. Sasaki, T. S. Kang, M.-a. Morikawa, B. Joarder, K. Moth-Poulsen, H. Bildirir, A. Mårtensson, N. Yanai, N. Kimizuka, *J Mat. Chem. C*, 2021, **9**, 11655–11661.

71 F. J. Morgan, H. Dugan, *Appl. Opt.*, 1979, **18**, 4112–4115.

72 A. Muratsugu, J. Watanabe, S. Kinoshita, *J. Chem. Phys.*, 2014, **140**, 214508.

73 A. Raj, P. Verma, A. Beliaev, P. Myllyperkiö, T. Kumpulainen, *Chem. Sci.*, 2025, **16**, 13935–13943.

74 F. Serra, E. M. Terentjev, *Macromolecules* 2008, **41**, 981–986.

75 M. W. Dale, D. J. Cheney, C. Vallotto, C. J. Wedge, *Phys. Chem. Chem. Phys.*, 2020, **22**, 28173–28182.

76 N. Gao, Y. Yang, Z. Wang, X. Guo, S. Jiang, J. Li, Y. Hu, Z. Liu, C. Xu, *Chem. Rev.*, 2024, **124**, 27–123.

77 L. V. T. D. de Alencar, S. B. Rodríguez-Reartes, F. W. Tavares, F. Llorell, *ACS Sustainable Chem. Eng.*, 2024, **12**, 7987–8000.

78 T. S. Kang, M.-a. Morikawa, M. Singh, N. Kimizuka, *J. Am. Chem. Soc.*, 2025, **147**, 8809–8819.

79 M. Mahato, Y. Murakami, S. K. Das, *Appl. Mater. Today*, 2023, **32**, 101808.

80 Y. Wang, *J. Phys. Chem. B*, 2009, **113**, 11058–11060. [View Article Online](#) [DOI: 10.1039/C9CP00212B](#)

81 J. Leier, N. C. Michenfelder, A.-N. Unterreiter, *Chem. Open*, 2021, **10**, 72–82.

82 K. P. Rola, A. Zajac, A. Szpecht, D. Kowal, J. Cybińska, M. Śmiglak, K. Komorowska, *Eur. Polym. J.*, 2021, **156**, 110615.

83 T. S. Groves, S. Perkin, *Faraday Discuss.*, 2024, **253**, 193–211.

84 I. Tanabe, Y. Kurawaki, Y. Morisawa, Y. Ozaki, *Phys. Chem. Chem. Phys.*, 2016, **18**, 22526–22530.

85 A. P. Demchenko, *Luminescence*, 2002, **17**, 19–42.

86 W. C. Galley, R. M. Purkey, *PNAS*, 1970, **67**, 1116–1121.

87 A. P. Demchenko, *Biophys. Chem.*, 1982, **15**, 101–109.

88 A. Paul, P. K. Mandal, A. Samanta, *J. Phys. Chem. B*, 2005, **109**, 9148–9153.

89 Z. Hu, C. J. Margulis, *Acc. Chem. Res.*, 2007, **40**, 1097–1105.

90 T. Singh, A. Kumar, *J. Phys. Chem. B*, 2008, **112**, 4079–4086.

91 Red-Edge Excitation Spectroscopy of Proteins with the FS5 Spectrofluorometer. Edinburgh Instruments Ltd. 2014

92 F. van Rantwijk, R. A. Sheldon, *Chem. Rev.*, 2007, **107**, 2757–2785.

93 I. Bandrés, M. Haro, B. Giner, H. Artigas, C. Lafuente, *Phys. Chem. Liq.*, 2011, **49**, 192–205.

94 H. Guo, Q. Yu, Y. Xiong, F. Yang, *J Mol. Liq.*, 2021, **335**, 116179.

95 C. Feng, K. Zhang, B. Zhang, L. Feng, L. He, C.-F. Chen, M. Li, *Angew. Chem. Int. Ed.*, 2025, **64**, e202425094.

96 G. Longhi, E. Castiglioni, J. Koshoubu, G. S. Abbate, *Chirality*, 2016, **28**, 696–707.

97 B. Zercher, T. A. Hopkins, *Inorg. Chem.*, 2016, **55**, 10899–10906.

98 Z. Huang, M. Yi, Y. Xu, P. Qi, Y. Liu, A. Song, J. Hao, *J. Mater. Chem. C*, 2021, **9**, 13276.

99 V. Morad, K. M. McCall, K. Sakhatskyi, E. Lehmann, B. Walfort, A. S. Losko, P. Trtik, M. Strobl, S. Yakunin, M. V. Kovalenko, *ACS Photonics*, 2021, **8**, 3357–3364.

100 T. Mizuta, K. Sueyoshi, T. Endo, H. Hisamoto, *Anal. Chem.*, 2021, **93**, 4143–4148.

101 S. Hisamitsu, N. Yanai, N. Kimizuka, *Angew. Chem. Int. Ed.*, 2015, **54**, 11550–11554.

102 S. Hisamitsu, N. Yanai, H. Kouno, E. Magome, M. Matsuki, T. Yamada, A. Monguzzi, N. Kimizuka, *Phys. Chem. Chem. Phys.*, 2018, **20**, 3233–3240.

103 S. Hisamitsu, J. Miyano, K. Okumura, J. K.-H. Hui, N. Yanai, N. Kimizuka, *Chem. Open*, 2020, **9**, 14–17.

104 K. Shimizu, S. Hisamitsu, N. Yanai, N. Kimizuka, J. N. C. Lopes, *J. Phys. Chem. B*, 2020, **124**, 3137–3144.

105 R. Kupfer, F. Wang, J. F. Wishart, M. Babzien, M. N. Polyanskiy, I. V. Pogorelsky, T. Rao, L. Cultrera, N. Vafaei-Najafabadi, M. A. Palmer, *Phys. Rev. Appl.*, 2023, **19**, 014052.

106 H. Zhang, C. Zhang, S. Vaziri, F. Kenarangi, Y. Sun, *IEEE Photonics J.*, 2021, **13**, 1500308.

107 A. N. Oraevsky, *Quantum Electron.*, 2002, **32**, 377.

108 T. Reynolds, N. Riesen, A. Meldrum, X. Fan, J. M. M. Hall, T. M. Monro, A. François, *Laser Photonics Rev.*, 2017, **11**, 1600265.

109 X. He, Q. Shao, P. Cao, W. Kong, J. Sun, X. Zhang, Y. Deng, *Lab Chip*, 2015, **15**, 1311–1319.

110 E. F. Borra, O. Seddiki, R. Angel, D. Eisenstein, P. Hickson, K. R. Seddon, S. P. Worden, *Nature*, 2007, **447**, 979–981.

111 E. Hecht (2001). Optics (4th ed.). Pearson Education

112 M. Tariq, M. G. Freire, B. Saramago, J. A. P. Coutinho, J. N. C. Lopes, L. P. N. Rebelo, *Chem. Soc. Rev.*, 2012, **41**, 829–868.

113 T. Szoboly, *Reflecting the future: Revolutionizing space exploration with liquid mirrors*. NC Space Grant News. 2024.

114 N. Rowlands, Á. Romero-Calvo, D. Strafford, R. Kamire, A. Childers, S. F. Yates, E. Rahislic, J. Smoke, S.-H. Zheng, P. Cameron, G. Cano-Gómez, H. Chen, T. Hu, E. Comstock, M. Herrada, *Proc. SPIE* 2024, 13100, Advances in Optical and Mechanical Technologies for Telescopes and Instrumentation VI, 131007H.



115 X. Hou, Z. Wang, Z. Zheng, J. Guo, Z. Sun, F. Yan, *ACS Appl. Mater. Interfaces*, 2019, **11**, 20417–20424

116 I. Bandrés, M. Haro, B. Giner, H. Artigas, C. Lafuente, *Phys. Chem. Liq.*, 2011, **49**, 192–205

117 H. Lin, P. W. Oliveira, M. Veith, *Appl. Phys. Lett.*, 2008, **93**, 141101

118 H. Lin, P. W. de Oliveira, M. Veith, *Opt. Mater.*, 2011, **33**, 759–762

119 Y. Chen, D. Zhao, Y. Bai, Y. Duan, C. Liu, J. Gu, X. Wang, X. Sun, Y. Li, L. Zhang, *J. Mol. Liq.*, 2022, **348**, 118031.

120 J. Luan, Y. Cheng, F. Xue, L. Cui, D. Wang, *ACS Omega*, 2023, **8**, 25582–25591

121 E. Ferreira, G. Ramos-Ortiz, A. Vazquez, M. Trejo-Durán, *J. Mol. Liq.*, 2023, **384**, 122253.

122 I. Betka, Nonlinear optical refractive index measurements of pure water via Z-scan technique at 800 nm, 2025, doi.org/10.48550/arXiv.2502.02944.

123 P. L. Rall, D. Förster, T. Graf, C. Pflaum, *Opt. Express*, 2022, **30**, 38643–38662.

124 S. M. Patil, S. K. Gupta, D. Goswami, R. Gupta, *ACS Omega*, 2023, **8**, 32444–32449

125 L. V. Elzen, T. A. Hopkins, *ACS Sustainable Chem. Eng.*, 2019, **7**, 16690–16697.

126 B. Nelson, L. V. Elzen, G. Whitacre, T. A. Hopkins, *ChemPhotoChem.*, 2021, **5**, 1071–1078

127 C. R. Wright, L. V. Elzen, T. A. Hopkins, *J. Phys. Chem. B*, 2018, **122**, 8730–8737.

128 Y. Murakami, S. K. Das, Y. Himuro, S. Maeda, *Phys. Chem. Chem. Phys.*, 2017, **19**, 30603–30615.

129 V. Khokhar, Deepika, S. Pandey, *Photochem. Photobiol. A: Chem.*, 2022, **427**, 113798.

130 Sangeeta, A. Sil, V. Singh, R. Bhati, B. Guchhait, *J. Phys. Chem. B*, 2024, **128**, 9805–9814

131 P. Zhou, K. Han, *Acc. Chem. Res.*, 2018, **51**, 7, 1681–1690

132 Z. Usmani, M. Sharma, M. Tripathi, T. Lukk, Y. Karpichev, N. Gathergood, B. N. Singh, V. K. Thakur, M. Tabatabaei, V. K. Gupta, *Sci. Total. Environ.*, 2023, **88**, 163002.

133 K. L. Kelly, E. Coronado, L. L. Zhao, G. C. Schatz, *J. Phys. Chem. B*, 2003, **107**, 668–677.

134 U. Banin, Y. Ben-Shahar, K. Vinokurov, *Chem. Mater.*, 2014, **26**, 97–110.

135 M. Bhar, N. Bhunia, G. H. Debnath, D. H. Waldeck, P. Mukherjee, *Chem. Phys. Rev.*, 2024, **5**, 011306.

136 J. Chang, H. Chen, G. Wang, B. Wang, X. Chena, H. Yuan, *RSC Adv.*, 2019, **9**, 7015–7024

137 T. Antrack, M. Kroll, M. Sudzius, C. Cho, P. Imbrasas, M. Albaladejo-Siguan, J. Benduhn, L. Merten, A. Hinderhofer, F. Schreiber, S. Reineke, Y. Vaynzof, K. Leo, *Adv. Sci.*, 2022, **9**, 2200379

138 F. Migliorini, S. Belmuso, R. Dondè, S. D. Iuliis, I. Altman, *Carbon Trend.*, 2022, **8**, 100184.

139 N. Tarasenka, A. Stupak, N. Tarasenka, S. Chakrabarti, D. Mariotti, *ChemPhysChem*, 2017, **18**, 1074–1083.

140 R. Jiang, Y. Guo, X. Guo, *Sol. Energy Mater. Sol. Cells*, 2026, **294**, 113934.

141 Y. U. Paulechka, A. G. Kabo, A. V. Blokhin, G. J. Kabo, M. P. Shevelyova, *J. Chem. Eng. Data*, 2010, **55**, 2719–2724

142 B. D. Rabideau, K. N. West, J. H. Davis, Jr., *Chem. Commun.*, 2018, **54**, 5019–5031.

143 P. Dehury, J. Singh, Tamal Banerjee, *ACS Omega*, 2018, **3**, 18016–18027.

144 E. Sperling, *Mapping the Impact of heat on photonics, Semiconductor Engineering* 2019, <https://semiengineering.com/mapping-the-impact-of-heat-on-light/>

145 Q. Jin, K. Williams, E. Yiwen, J. Dai, and X. -. Zhang, "Observation of broadband terahertz wave generation from liquid water," in *Nonlinear Optics*, OSA Technical Digest (online) (Optica Publishing Group, 2017), paper NW3A-1, doi:10.1364/OFC-17-4142B

146 Q. Jin, Y. W. E, J. M. Dai, L. L. Zhang, C. L. Zhang, A. Tcyplkin, S. Kozlov, and X. -. Zhang, "Terahertz photonics in liquids," in *Nonlinear Optics (NLO)*, OSA Technical Digest (Optica Publishing Group, 2019), paper NTU2B.3.

147 P. Q. Liu, X. Miao, S. Datta, *Opt. Mater. Express*, 2023, **13**, 699–727.

148 P. C. Wu, T.-H. Kim, A. S. Brown, M. Losurdo, G. Bruno, and H. O. Everitt, *Appl. Phys. Lett.*, 2007, **90**, 103119.

149 C. Kunkel, J. T. Margraf, K. Chen, H. Oberhofer, K. Reuter, *Nat. Commun.*, 2021, **12**, 2422.

150 C. Wang, H. Dong, L. Jiang, W. Hu, *Chem. Soc. Rev.*, 2018, **47**, 422–500.

151 A. Chelsea, Are Liquid Solar Panels the Next Big Thing in Solar Power? *Green Lancer*, 2024, <https://www.greenlancer.com/post/liquid-solar>

152 P. V. Kamat, K. Tvrdy, D. R. Baker, E. J. Radich, *Chem. Rev.*, 2010, **110**, 6664–6688

153 T. Ullrich, D. Munz, D. M. Guldi, *Chem. Soc. Rev.*, 2021, **50**, 3485–3518.

154 P. Bharmoria, H. Bildirir, K. Moth-Poulsen, *Chem. Soc. Rev.*, 2020, **49**, 6529–6554.

155 V. Sharma, R. Suthar, S. Karak, A. Sinha, *ACS Appl. Opt. Mater.*, 2025, **3**, 259–271.

156 W. G.J.H.M. van Sark, K. W. J. Barnham, L. H. Slooff, A. J. Chatten, A. Büchtemann, A. Meyer, S. J. McCormack, R. Koole, D. J. Farrell, R. Bose, E. E. Bende, A. R. Burgers, T. Budel, J. Quilitz, M. Kennedy, T. Meyer, C. D. M. Donegá, A. Meijerink, D. Vanmaekelbergh, *Opt. Express*, 2008, **16**, 21773–21792.

157 L. Naimovičius, P. Bharmoria, K. Moth-Poulsen, *Mater. Chem. Front.*, 2023, **7**, 2297–2315.

158 B. Daiber, K. van den Hoven, M. H. Futscher, B. Ehrler, *ACS Energy Lett.*, 2021, **6**, 2800–2808.

159 D. Nguyen, T. Van Huynh, V. S. Nguyen, P.-L. D. Cao, H. T. Nguyen, T.-C. Wei, P. H. Tran and P. T. Nguyen, *RSC Adv.*, 2021, **11**, 21560–21566.

160 D. Nguyen, M. T. Nguyen, T. T. D. Nguyen, V. T. Huynh, B. P. N. Nguyen and P. T. Nguyen, *Aust. Ceram. Soc.*, 2022, **58**, 913–921.

161 M. Gorlova, L. K-161loo, *Dalton Trans.*, 2008, 2655–2666.

162 M. Hassan, T. A. Shifa, A. Vomiero, E. Moretti, K. B. Ibrahim, *Small* 2025, **21**, e09030.

163 S. Fernandes, J.C.G.E. da Silva, L.P. da Silva, *Materials*, 2022, **15**, 3446.

164 C. Yang, H. A. Atwater, M. A. Baldo, D. Baran, C. J. Barile, M. C. Barr, M. Bates, M. G. Bawendi, M. R. Bergren, B. Borhan, C. J. Brabec, S. Brovelli, V. Bulovic, P. Ceroni, M. G. Debije, J.-M. Delgado-Sanchez, W.-J. Dong, P. M. Duxbury, R. C. Evans, S. R. Forrest, D. R. Gamelin, N. C. Giebink, X. Gong, G. Griffini, F. Guo, C. K. Herrera, A. W. Y. Ho-Baillie, R. J. Holmes, S. -K. Hong, T. Kirchartz, et al., *Joule*, 2022, **6**, 8.

165 M. Mokhtarpour, A. Rostami, H. Shekaari, A. Zarghami, S. Faraji, *Sci. Rep.*, 2023, **13**, 18936.

166 S. L. Piper, M. Kar, D. R. MacFarlane, K. Matuszek, J. M. Pringle, *Green Chem.*, 2022, **24**, 102–117.

167 M. Królikowski, M. Więckowski, K. Źółtańska, M. Królikowska, *J. Chem. Eng. Data*, 2024, **69**, 958–972.

168 Z. Wang, A. Roffey, R. Losantos, A. Lennartson, M. Jevric, A. U Petersen, M. Quant, A. Dreos, X. Wen, D. Sampedro, K. Börjesson, K. Moth-Poulsen, *Energy Environ. Sci.*, 2019, **12**, 187–193.

169 Z. Wang, H. Hözel, K. Moth-Poulsen, *Chem. Soc. Rev.*, 2022, **51**, 7313–7326.

170 X. Xu, G. Wang, *Small*, 2022, **18**, e2107473.

171 X. Xu, C. Li, W. Li, J. Feng, W.-Y. Li, *Energy Environ. Sci.*, 2025, **18**, 8990–9017.

172 N. Baggi, H. Hözel, H. Schomaker, K. Moreno, K. Moth-



ARTICLE

Journal Name

Poulsen, *ChemSusChem*, 2023, **17**, ge202301184.

173 N. Baggi, L. M. Muhammad, Z. Liasi, J. L. Elholm, P. Baronas, E. Molins, K. V. Mikkelsen, K. Moth-Poulsen, *J. Mater. Chem. A*, 2024, **12**, 26457-26464.

174 L. Fernandez, H. Hözel, P. Ferreira, N. Baggi, K. Moreno, Z. Wang, K. Moth-Poulsen, Surfactant-enabled strategy for molecular solar thermal energy storage systems in water. *Green Chem.*, 2025, **27**, 14119-14130.

[View Article Online](#)
DOI: 10.1039/D5CP04142B



All figures presented in this manuscript have been prepared by the authors themselves and any information related to drawing is available with the corresponding author with a reasonable request by email. Appropriate references have cited where needed in relation to the presented figures.

[View Article Online](#)
DOI: 10.1039/DSCP04142B

